Microbiome

RESEARCH

Open Access

Sex-specific responses of *Taxus mairei* to UV-B radiation involved altering the interactions between the microbiota assembly and host secondary metabolism

Hongshan Zhang[1,2†], Kailin Hou[1†], Xueshuang Liang[1], Wanting Lin[1], Ruoyun Ma[1], Yue Zang[1], Xiaori Zhan[1], Mingshuang Wang[1], Shangguo Feng[1], Qicai Ying[1], Bingsong Zheng[3], Huizhong Wang[1] and Chenjia Shen[1,2*]

Abstract

Background To adapt to constantly changing environments, ancient gymnosperms have coevolved with diverse endophytic fungi that are essential for the fitness and adaptability of the plant host. However, the effect of sex on plant-endophyte interactions in response to environmental stressors remains unknown. RNA-seq integrated with ITS analysis was applied to reveal the potential mechanisms underlying the sex-specific responses of *Taxus mairei* to ultraviolet (UV)-B radiation.

Results Enrichment analysis suggested that sex influenced the expression of several genes related to the oxidation–reduction system, which might play potential roles in sex-mediated responses to UV-B radiations. ITS-seq analysis clarified the effects of UV-B radiation and sex on the composition of endophytic fungal communities. Sex influenced various secondary metabolic pathways, thereby providing chemicals for *T. mairei* host to produce attractants and/or inhibitors to filter microbial taxa. Analysis of fungal biomarkers suggested that UV-B radiation reduced the effect of sex on fungal communities. Moreover, *Guignardia* isolate #1 was purified to investigate the role of endophytic fungi in sex-mediated responses to UV-B radiation. Inoculation with spores produced by isolate #1 significantly altered various oxidation–reduction systems of the host by regulating the expression of *APX2*, *GST7 NCED1*, *ZE1*, *CS1*, and *CM1*.

Conclusion These results revealed the roles of endophytic fungi in sex-mediated responses to UV-B radiation and provided novel insights into the sex-specific responses of *Taxus* trees to environmental stressors.

Keywords Dioecious plant, Fungal community, *Guignardia*, Oxidation–reduction system, *Taxus*, UV-B radiation

Introduction

Sex differentiation of plants plays a significant role in the utilization and allocation of resources for biological functions, such as metabolism and reproduction [1]. Unlike animals, most plants are monoecious [2]. Gymnosperms are the most representative species of dioecious plants and, therefore, considered good specimens for the study of genetic sex determination and sexual phylogeny [3]. For example, a natural population of *Pinus bungeana*, an endemic conifer, was used to reveal the role of sexual identity in the reproductive

†Hongshan Zhang and Hou Kailin contributed equally to this work.

*Correspondence:
Chenjia Shen
shencj@hznu.edu.cn
[1] College of Life and Environmental Sciences, Hangzhou Normal University, Hangzhou 310036, China
[2] Kharkiv Institute, Hangzhou Normal University, Hangzhou 311121, China
[3] State Key Laboratory of Subtropical Silviculture, Zhejiang A&F University, Hangzhou 311300, China

organs of plants [3], while Ginkgo, an ancient lineage of dioecious gymnosperms, was used to identify the sex-determining region on chromosome 2 by screening four MADS-box genes related to sex determination [2].

Sexual dimorphism has been widely reported in morphology, physiology, gene expression, and immunity [4]. In addition, significant differences in the accumulation of secondary metabolites were found between female and male trees [5]. An investigation of the dioecious willow reported the identification of various sexually dimorphic volatile and non-volatile floral secondary metabolites [6]. Furthermore, *Ginkgo biloba* was used to investigate the effects of genetic sex on flavonoid-specific metabolism and regulation [2]. Drought stress was found to cause massive accumulation of defensive metabolites, such as flavonoids, iso-flavonoids, neo-flavonoids, and alkaloids [7]. A recent study also showed that sex affects microbiome assemblies of plants under various stress conditions [8]. In natural *Populus euphratica* forests, the sex-specific impacts on microbial communities were investigated by sequencing of internal transcribed spacers (ITSs) [9]. The proportions of several nitrogen-fixing microbes, such as members of the genera *Brevundimonas* and *Microvirga*, are enriched in the roots of male papaya trees [10]. Significant differences in the relative abundance of phyla *Ascomycota* and *Basidiomycota* were observed between female and male trees of the dioecious species *Populus cathayana* [11]. Furthermore, a close relationship between root phenolic metabolites is reportedly closely related to sex-related bacterial communities in *P. euphratica* [12].

Typically, sexual dimorphism is thought to be the result of environmental stress [13, 14]. Differential reproductive costs may lead to different responses of female and male plants to environmental stressors [15]. Females commonly exhibit greater responsiveness and are more negatively impacted under various stress conditions, including elevated CO_2 levels, drought, pathogen infection, and reduced soil fertility [16–18]. Exposure to ultraviolet (UV)-B radiation is an important environmental factor that significantly affects the development process, physiological and biochemical characteristics, as well as secondary metabolism of plants [19]. Numerous studies have demonstrated that low-intensity UV-B radiation effectively promotes the production of secondary metabolites in plant tissues. For example, Li's group clarified the transcriptional regulation mechanism of UV-B-induced production of artemisinin and flavonoids [20]. Jiao's group revealed the mechanisms underlying the biosynthesis of flavonoids and taxane in *T. cuspidate* in response to UV-B radiation [21].

Taxus mairei is a relict species originating from ancient quaternary glaciers and mainly distributed in eastern and southern China [22, 23]. As a medicinal tree, *T. mairei* produces various natural ingredients with anticancer activities, such as Taxol and its derivatives [24]. Modern medical studies have confirmed that Taxol can be used to treat various types of cancers, such as ovarian, lung, and esophageal cancers [25]. The significant medicinal value of Taxol has led to massive illegal logging, thus endangering wild populations of wild *Taxus* trees [26, 27]. Enhancing the adaptability to environmental factors is an essential approach to protect and expand the wild populations of *T. mairei*.

The responses of *T. mairei* to various environmental conditions, including UV-B radiation, have been extensively studied. Various factors, such as leaf traits, gas exchange rates, pigment contents, and cellular defenses, participate in the responses of *Taxus* trees to UV-B radiation [28]. A number of genes associated with the biosynthesis of flavonoid and taxoid were up-regulated in *T. cuspidata* plantlets in response to UV-B radiation [21]. Plants provide an environment for endophytic fungi, while endophytic microorganisms participate in nutrient synthesis, affect growth and development, inhibit the growth of competitors, and improve stress resistance [29]. Many endophytic fungi from *Taxus* trees have been isolated and identified in the past decades [30, 31]. Previous studies have focused on screening of taxol-producing fungi, while research on fungi responsive to environmental stress remains limited. Here, the effect of sex on the responses of *T. mairei* to UV-B radiation was investigated by ITS-seq and transcriptomic analyses. Various endophytic fungi have been isolated and cultured from *T. mairei*, thereby providing a foundation to study the impact of endophytic fungi on sex-mediated stress responses. Our data provides new insights into the sex-specific responses of *Taxus* trees to environmental stressors.

Materials and methods

Plant materials and treatments

In the present study, female and male *T. mairei* trees were separately selected and planted at the experimental field of Hangzhou Normal University, Hangzhou, China. All trees were placed in pots (30 cm in diameter and 20 cm in height) for cultivation at day/night temperature 22 ~ 25 ℃/15 ~ 18 ℃ and photoperiod of 12 h.

All the trees were classed into four independent groups. Four groups were set up in the present experiment as follows: male trees under control condition (M_0 h), female trees under control condition (F_0 h), male trees under UV-B radiation for 48 h (M_48 h), and female trees under UV-B radiation for 48 h (F_48 h). UV-B radiation was

artificially produced by a UV-B fluorescent lamp (40 W, λmax = 313 nm, Electric Light Source Research Institute, Beijing, China). The distance between the UV-B lamp and the plant sample was adjusted to keep it under low-intensity radiation (3 W/m^2), which was determined by an ultraviolet photometer (Spectrum Technologies). After radiation treatment, the twigs of *T. mairei* were harvested and frozen in liquid N_2 and kept at − 80 ℃ for DNA and RNA extraction. Five independent male and female trees were used for ITS analysis and three independent male and female trees were used for transcriptome analysis.

RNA extraction and cDNA library construction

Total RNAs were isolated using TRIzol reagent (ThermoFisher) following its protocol. RNAs with a RIN number > 7.0 were collected to construct the cDNA library. The quantity and purity of total RNAs were analyzed using the Bioanalyzer 2100 a (Agilent, CA, USA, 5067–1511). Utilizing Nanobeads Oligo-dT (Thermo Fisher, CA, USA), mRNAs were purified and broken up into small fragments using a divalent cation and a high-temperature RNA fragmentation buffer (NEB, USA). The purified RNA fragments were harvested to synthesize second-stranded DNAs by SuperScript™ II Reverse Transcriptase kit (Invitrogen, USA). The resulting second-stranded cDNAs were treated with the heat-labile enzyme (NEB, USA) and amplified with PCR.

Filtering of clean reads and sequence alignment

Twelve cDNA libraries (three repeats for each group) from the pooled RNA from twig samples of *T. mairei* were sequenced on with Illumina NovaSeq™ 6000 sequencing platform, generating a number of 150 bp paired-end reads. High-quality clean reads were filtered by Cutadapt software according to default parameters. Several quality parameters, including the Q20, Q30, and GC content, were analyzed using FastQC software. All reads were aligned onto the *T. mairei* reference genome using the HISAT2 package [32].

Gene annotation and differentially expressed genes (DEGs) analysis

For gene function annotation, all referring protein sequences were aligned by the BLASTX program against different protein databases. Expression analysis was performed using DESeq2 software. The genes with false discovery rate (FDR) < 0.05 and absolute fold change ≥ 2 were treated DEGs. Within the DEG pools, GO and KEGG enrichment analysis was performed with a two-tailed Fisher's exact test.

DNA extraction and ITS amplification

Total DNA from different samples was extracted using the cetyltrimethylammonium bromide method. The resulting DNA was PCR amplified by LC-Bio Technology Co., Ltd. (Hangzhou, China). The primers ITS1FI2 (5′-GTGARTCATCGAATCTTTG-3′) and ITS2 (5′-TCCTCCGCTTATTGATATGC-3′) were used for the internal transcribed spacer region (ITS2) sequencing. After purification and quantification, the PCR products were prepared for ITS sequencing on the NovaSeq PE250 platform according to its instructions.

Paired-end reads were assigned to samples by cutting off the barcodes and primers. high-quality clean tags were quality filtered using the raw reads using Fqtrim software (ver. 0.94). Chimeric sequences were filtered using Vsearch software (ver. 2.3.4) and were dereplicated using the DADA2 package (ver. 1.8). Alpha and beta diversities were calculated by QIIME2 with R (ver. 3.5.2), and the relative abundance (fungi count/total count) was used to determine fungi taxonomy. The sequence annotation was performed by the QIIME2 plugin feature classifier according to the alignment database. The Pearson correlation coefficient among different replicates was calculated to evaluate the reliability and stability of experimental data. Principal component analysis (PCA) was performed using the Princomp function of R (ver. 3.5.2).

ITS sequence data analysis

The compositional changes among endophytic fungus communities were analyzed by the principal coordinates analysis (PCoA) according to Bray–Curtis distances. A one-way analysis of similarity (ANOSIM) was applied to measure the effects of sex and UV-B treatment on the endophytic fungus communities and gene expression. The Linear discriminant analysis coupled with the effect size analysis (LEfSe) ($P < 0.05$) was used to analyze the effect of sex and/or UV-B treatment on the relative abundance of fungal taxa from phyla to genera. Due to no longer relying on the OTU information input format, PICRUSt2 can be used not only for functional prediction of 16 s bacteria and archaea, but also for functional prediction of 18S, ITS fungi, and algae. PICRUSt2 was used to predict the function of the fungal community in the different sample groups [33].

Untargeted metabolomic profiling

Metabolite exaction was performed according to our previous study [34]. The *T. mairei* extracts were fractioned on Waters ACQUITY UPLC I-Class plus system with ACQUITY UPLC HSS T3 (100 mm × 2.1 mm, 1.8 μm) column. The obtained metabolites were

determined by a high-resolution MS/MS TripleTOF 5600 Plus System (Sciex, UK) with default operation parameters [34].

The analysis of MS data parameters, such as peak picking, peak grouping, and peak annotation, was performed using XCMS software. The MS data was processed to identify different features, such as baseline, peak recognition, retention time (RT), and peak alignment and normalization, using Progenesis QI software (ver. 3.0, Nonlinear Dynamics, Newcastle, UK). The identification of compounds is based on multiple dimensions, such as RT, precise mass number, secondary fragments, and isotopes. The Lipidmaps (ver. 2.3), METLIN database, and LuMet Plant3.0 local database were used for identification analysis.

Isolation of endophytic fungi

The *T. mairei* samples were surface washed twice in ddH_2O to remove extraneous impurities and sterilized by immersion in 75% ethanol for 2 min followed by 1.5% sodium hypochlorite for 5 min. Surface sterilized tissue samples were kept on PDA media adding 30 μg/mL streptomycin sulphate at 26 ℃ under 12 h of light/dark cycles. The emerging fungi were transferred to fresh PDA media to obtain the pure cultures. Based on their colony morphology, cultures were treated as different isolates with unique IDs.

Molecular characterization of endophytic fungal isolates

The total genomic DNAs of all endophytic fungal isolates were extracted by the CTAB method. To characterize the selected endophytic fungal isolates, the ITS region of genomic DNA was amplified using classic ITS1/4 primers (5′-TCCGTAGGTGAACCTGCGG-3′/5′-TCCTCCGCTTATTGATATGC-3′). The amplified products were sequenced and the resulting DNA sequences were searched against the NCBI GenBank database. Three parameters, including identity, maximum query, and score, were used to identify the endophytic fungus.

Determination of melanin from endophytic fungal isolates

A microorganism melanin ELISA Kit was used for the determination of melanin from the selected endophytic fungal isolates according to its assay procedure. Briefly, a series of 50 μL standards in different concentrations were added to each hole. Then, 10 μL of experimental samples were added to the sample holes and 100 μL of Horseradish Peroxidase labeled detection antibody was added to all holes, except for the blank hole, at 37 ℃ in the dark for 15 min. After discarding the working liquid, all holes were washed twice with washing solution. At last, 50 μL of termination solution was added to each hole, and the OD value was determined at a wavelength of 450 nm.

Artificial infection of endophytic fungus

The twigs were surface washed twice with ddH_2O ($N=3$ for each group), and then sprayed with 2 mL spore suspension (1×10^6 spores/mL) of the endophytic fungus (*Guignardia* isolate #1). Another twig group sprayed with ddH_2O without spore was treated as a control. After 2 days of incubation, the infection area of each twig was washed by ddH_2O twice and harvested for further analysis.

Real-time PCR validation

Total RNAs from the control and *Guignardia* isolate #1-treated sample were isolated by a Plant RNeasy Mini kit (Qiagen, Hilden, Germany) according to its instructions. Three independent samples for each group were used. DNase I enzyme was used to remove genomic DNA contamination. The cDNA was synthesized by ReverAid First Strand cDNA Synthesis Kit (Thermo Scientific, Shanghai, China). QRT-PCR was performed using the SYBR Premix Ex Taq Kit (TaKaRa, Dalian, China) and a DNA Sequence Detection System (ABI PRISM 7700, Applied Biosystems, Shanghai, China). An ACTIN sequence was used as the internal standard gene to calculate relative fold differences by the values of comparative cycle threshold ($2^{-\Delta\Delta Ct}$). All the primer sequences are listed in Table S1.

Results

Overview of the RNA-seq and ITS-seq datasets

To identify the responses of *T. mairei* to UV-B radiation, integrated RNA-seq and ITS-seq analysis was performed (Fig. 1a). RNA-seq produced a total of 516,065,236 clean reads, amounting to 77.4 Gb of sequence data. About 99.99% and 97.82% of the clean reads had quality scores at the Q20 and Q30 levels, respectively. The average GC content of all reads was 44.0% (Table S2). More than 90% of the reads were mapped to the *T. mairei* reference genome, with less than 5% being multiple mapped (Table S3). The percentages of PC1 and PC2 were 85.34% and 7.74%, respectively, suggesting dramatic variations among the different sample groups (Fig. 1b). The results of correlation analysis confirmed that the experiments were reliable (Figure S1). ITS-seq produced 1,676,434 raw tags, of which 1,558,748 were valid tags. After filtering, about 99.43% and 98.12% of the clean sequences obtained scores at the Q20 and Q30, respectively (Table S4). The average GC content was 54.52%. Differential mobility spectrometry analysis confirmed significant differences in the fungal communities among the four sample groups (Fig. 1c).

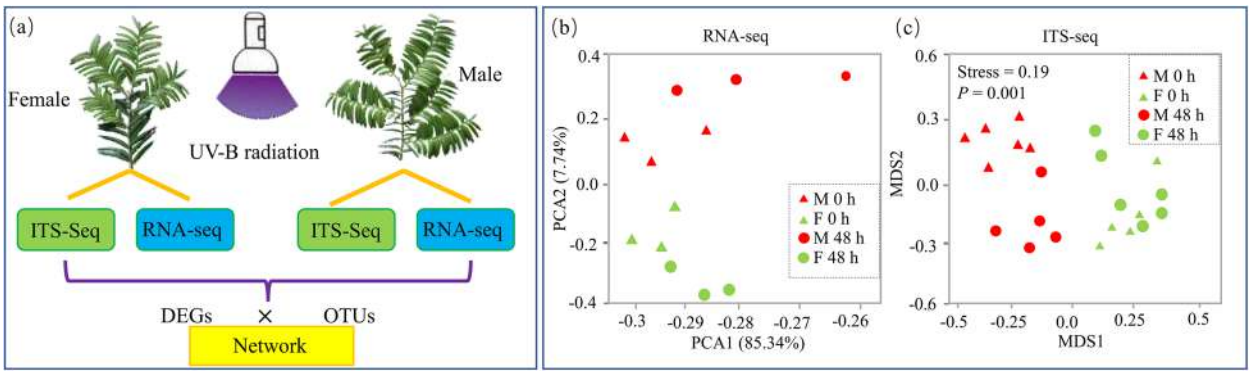

Fig. 1 Analysis of the responses of female and male *T. mairei* trees to UV-B radiation. **a** The workflow of integrated RNA-seq and ITS-seq analysis of the female and male *T. mairei* trees under UV-B radiation. **b** Principal component analysis of the RNA-seq datasets from different sample groups. **c** Dynamic meta-storms analysis of the ITS-seq datasets from different sample groups

Analysis of the DEGs in response to UV-B radiation

Based on the FPKM data, the expression profiles are illustrated with a heatmap (Figure S2a). The numbers of DEGs identified by four comparisons, namely F_48/0 h, M_48/0 h, F/M_0 h, and F/M_48 h, are depicted in a Venn diagram (Figure S2b). In detail, 4118 up- and 4281 downregulated genes were identified by the F_48/0 h comparison, 3816 up- and 3885 downregulated genes by the M_48/0 h comparison, 947 up- and 874 downregulated genes by the F/M_0 h comparison, and 761 up- and 699 downregulated genes by the F/M_48 h comparison (Figure S2c). After filtering of all unknown genes, the zinc finger *ZAT9* gene (ctg2987_gene.5), *PAM68* gene (ctg1018_gene.1), and the biopterin transport protein-encoding gene (ctg11372_gene.4) were identified as the top three most significant UV-B responsive genes in the female trees (Table S5). In the male trees, the top three significant UV-B responsive genes were the receptor-like protein-encoding gene (ctg11872_gene.6), UDP-glycosyltransferase encoding gene (ctg4164_gene.4), and AP2/ERF and B3 domain-containing transcription repressor TEM1 encoding gene (ctg1208_gene.7) (Table S6).

Enrichment analysis of DEGs responsive to UV-B radiation

Most of the DEGs responsive to UV-B radiation were assigned to at least one GO term. In both female and male trees, several environmental response-related GO terms were associated with a number of DEGs, such as "oxidation–reduction process" (GO:0055114), "defense response" (GO:0006468), and "response to oxidative stress" (GO:0006979) (Figure S3). To reveal the effect of sex on the responses of *T. mairei* to photo-stress, eight photo-responsive GO terms, including "photoprotection", "cellular response to light stimulus", "response to light stimulus", "response to UV-B", "response to red light", "red or far-red light signaling", "photosystem I", and "photosystem II", were selected for analysis of significance. For the selected GO terms, the *P* values of the female trees were smaller than those of the male trees in response to UV-B radiation, suggesting that the DEGs of the female trees were significantly enriched in GO terms related to photo-stress (Fig. 2a). The number of DEGs also confirmed that female trees had a slightly stronger response to light stress (Fig. 2b).

To reveal the differential metabolic responses of *T. mairei* trees to UV-B radiation, all DEGs were assigned to various KEGG pathways. Significance analysis showed that most UV-B responsive genes were enriched in KEGG pathways associated with amino acids, secondary metabolites, carbohydrates, environmental adaptation and energy, and terpenoids (Fig. 2c). The number of DEGs in each significantly enriched KEGG pathway was counted. Interestingly, most of the DEGa related to galactose and sulfur were down-regulated in both female and male trees. Most of the DEGs associated with tryptophan metabolism, photosynthesis, brassinosteroid biosynthesis, and monoterpenoid biosynthesis were up-regulated in both the female and male trees. However, most of the photosynthesis-related DEGs were identified in the female trees rather than the male trees (Fig. 2d).

Enrichment analysis of sex-related DEGs

In total, 1820 and 1460 sex-related DEGs were identified by the F/M 0 h and F/M 48 h comparisons, respectively, which included 166 DEGs detected by both comparisons (Fig. 3a), suggesting that sexual dimorphism was altered by exposure to UV-B radiation. GO enrichment analysis showed that sexual dimorphism of *T. mairei* under the control conditions was associated with several environmental stress-related GO terms, such as "response to cold" and "photoprotection". In response to UV-B radiation, most of the DEGs were enriched in various

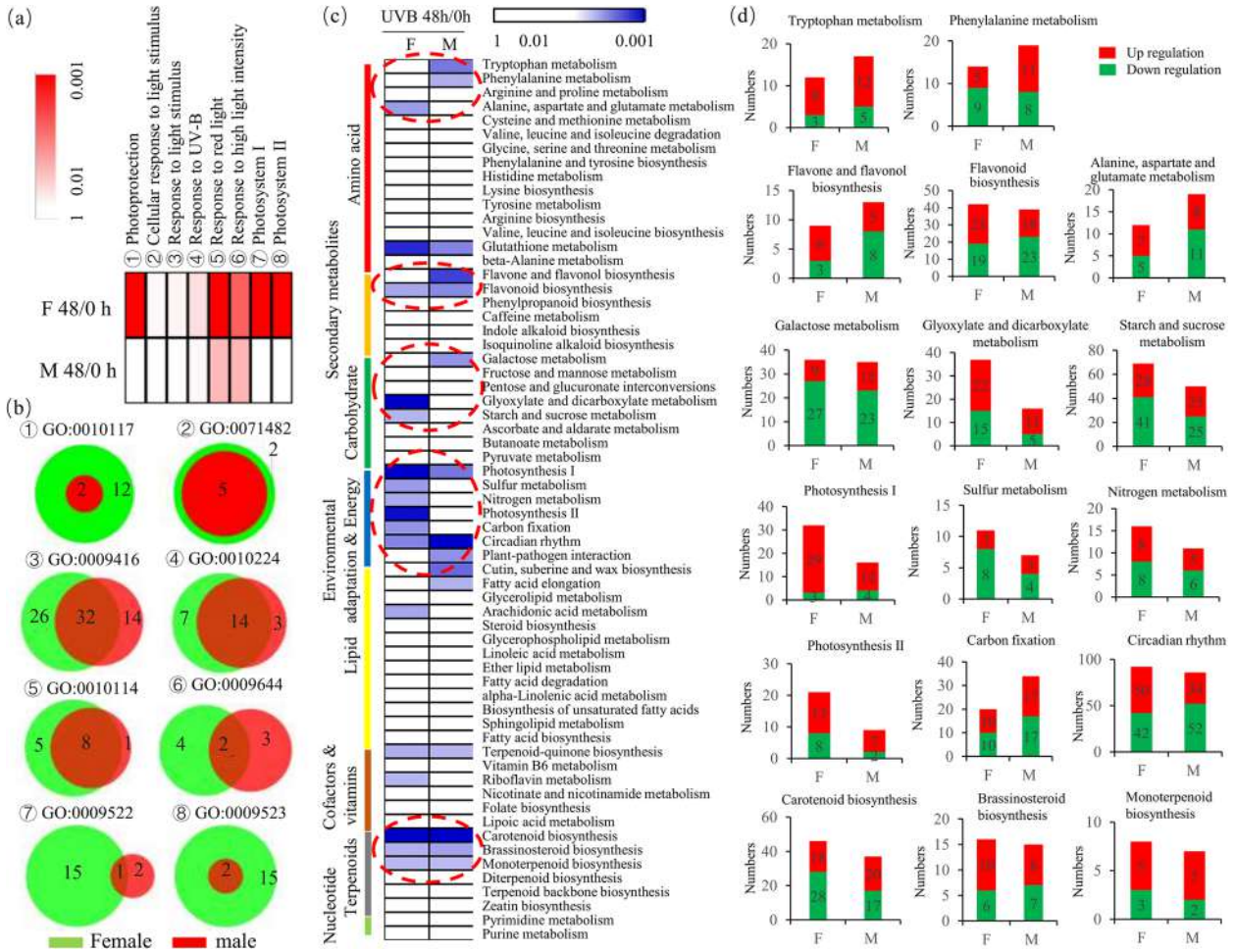

Fig. 2 Enrichment analysis of the DEGs responsive to UV-B radiation. **a** Significance analysis of eight photo-responsive GO terms in both female and male trees. Red color indicated the significance $P < 0.01$. **b** The number of DEGs assigned to eight photo-responsive GO terms. Green cycles indicated the DEGs in the female trees and red cycles indicated the DEGs in the male trees. **c** Significance analysis of various metabolism-related KEGG pathways. The blue color indicated the significance value $P < 0.01$. Red dashed circles indicated the enriched KEGG pathways. **d** The number of DEGs in each significantly enriched KEGG pathway. Red indicates the number of up-regulated genes and green indicates the number of down-regulated genes

metabolism-related GO terms, such as "starch metabolic process" and "flavonoid biosynthetic process" (Fig. 3b).

To reveal the differential metabolic pathways between female and male trees, all DEGs were assigned to KEGG pathways. Under the control conditions, there were significant differences in metabolism-related KEGG pathways between the female and male trees. In response to UV-B radiation, metabolism-related differences were greatly reduced. For example, the only KEGG pathways significantly enriched in the F/M 0 h comparison were "beta-alanine metabolism", "indole alkaloid biosynthesis", "glycerolipid metabolism", "glycerophospholipid metabolism", and "fatty acid degradation" (Fig. 3c). Notably, only three KEGG pathways, including "phenylalanine and tyrosine biosynthesis", "glutathione metabolism", and "carotenoid biosynthesis", were significantly enriched by the F/M 48 h comparison. In detail, six "phenylalanine and tyrosine biosynthesis" pathway-related genes, 19 "glutathione metabolism" pathway-related genes, and 18 "carotenoid biosynthesis" pathway-related genes were identified between the female and male trees after exposure to UV-B radiation for 48 h, suggesting potential roles in sex-mediated responses to UV-B radiation (Fig. 3d–f).

Differentially expressed TFs between the female and male trees

Along with the 1,460 DEGs identified by the F/M 48 h comparison, 10 differentially expressed TFs were also identified (Table S7). After exposure to UV-B radiation for 48 h, *RAV1* (ctg9799_gene.4), *TEM1.1*

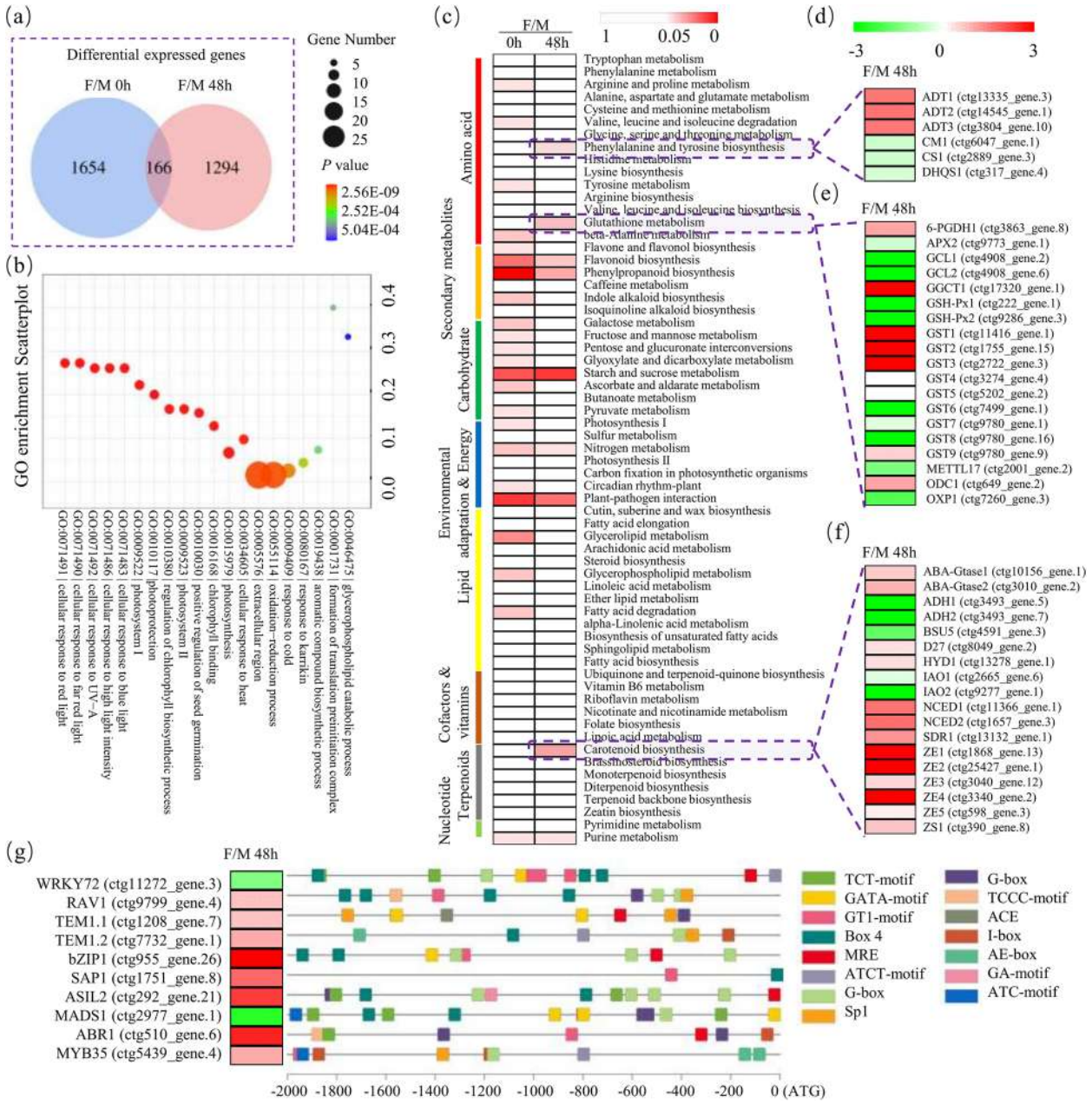

Fig. 3 Enrichment analysis of the DEGs between female and male trees. **a** Venn diagram showing the number of sex-related DEGs under UV-B radiation. **b** Enrichment analysis of the sex-related DEGs in several environmental stress-related GO terms. **c** The differential response of metabolic pathways between the female and male trees. Red color indicates the significance value $P < 0.01$. **d** Expression levels of phenylamine and tyrosine biosynthesis-related genes. **e** Expression levels of glutathione metabolism-related genes. **f** Expression levels of carotenoid biosynthesis-related genes. Red indicated up-regulated genes and green indicated down-regulated genes. The heatmap scale ranges from − 3 to + 3 on a $\log_2$ scale. **g** Analysis of the light-responsive *cis*-elements in upstream promoter sequences of differentially expressed TF genes. Different color boxes indicated various light-responsive *cis*-elements

(ctg1208_gene.7), *TEM1.2* (ctg7732_gene.1), *bZIP1* (ctg955_gene.26), *SAP1* (ctg1751_gene.8), *ASIL2* (ctg292_gene.21), *ABR1* (ctg510_gene.6), and *MYB35* (ctg5439_gene.4) highly expressed in the female trees, while *WRKY72* (ctg11272_gene.3) and *MADS1* (ctg2977_gene.1) were comparatively up-regulated in the male trees.

To identify *cis*-elements responsive to light, promoter sequences located 2000 bp upstream were extracted from the *T. mairei* genome. In total, 15 light response-related

cis-elements were used to screen the full promoters of TF genes responsive to UV-B radiation. Several TF promoters contained more than 10 light response-related *cis*-elements. For example, the promoter of *WRKY72* (ctg11272_gene.3) had 13 light-responsive *cis*-elements, such as three TCT-motifs, one GATA-motif, three GT1-motifs, three Box 4 s, one MRE, one ATCT-motif, and one G-box, while the promoter of *MADS1* (ctg2977_gene.1) had 11 light responsive *cis*-elements, such as two Box-4 s, one GA-motif, five G-boxes, one MRE, and two TCT-motifs (Fig. 3g). Our data suggest that these potential light responsive TFs might be involved in sex-mediated responses to UV-B radiation.

Differences in community structures of endophytic fungi

The endophytic fungal communities in *T. mairei* trees were significantly affected by both sex and exposure to UV-B radiation (Fig. 4a, b). Furthermore, alpha and beta diversity analysis confirmed the effects of sex and UV-B radiation on the fungal communities (Figure S4). Furthermore, the results of hierarchical clustering analysis suggested that samples from the 0 and 48 h groups were

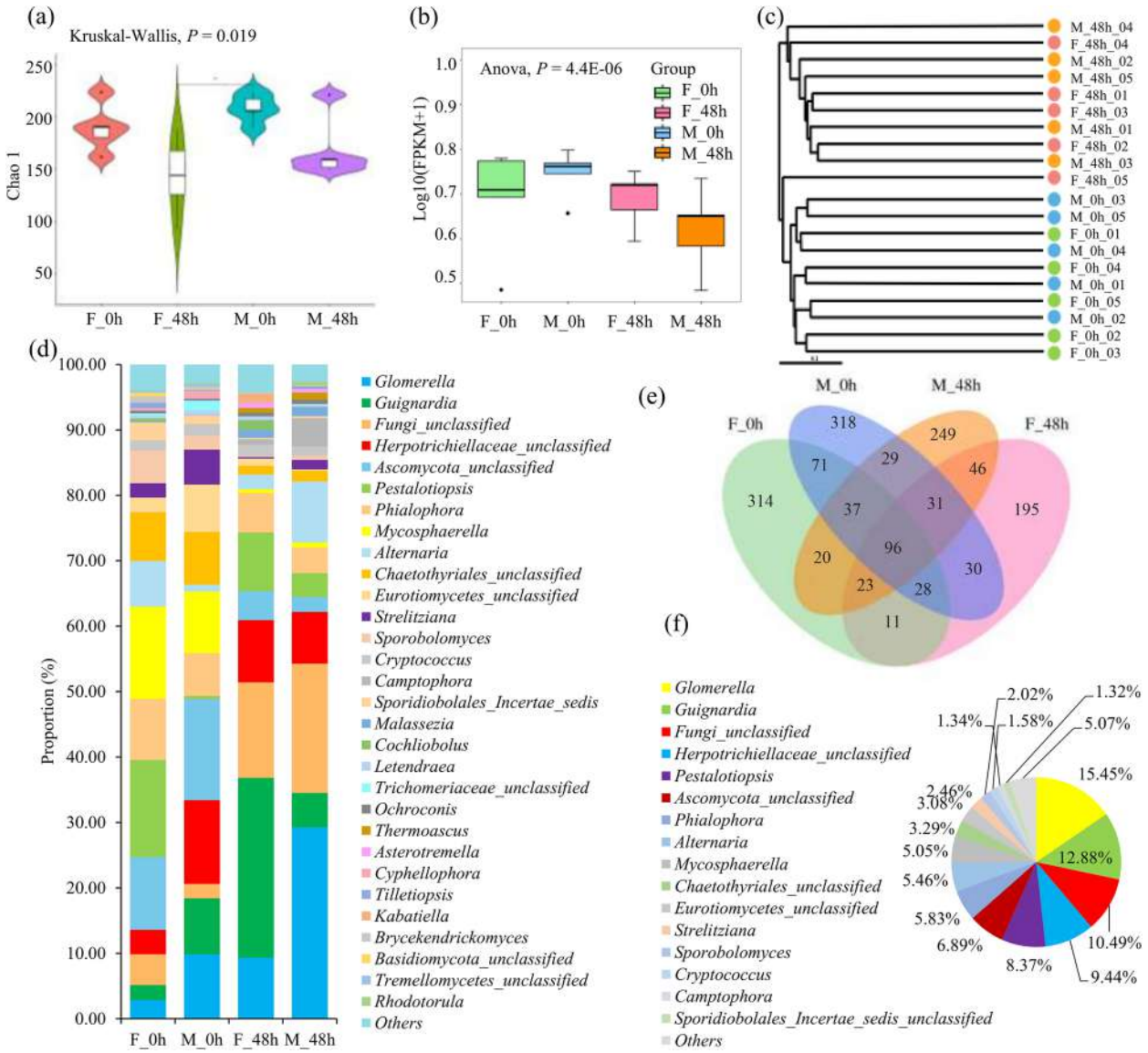

Fig. 4 Differences in community structure of endophytic fungi. **a** Analysis of alpha diversity by Chao1 index. **b** Analysis of alpha diversity by Shannon index. **c** Analysis of beta diversity by upgma clustering. **d** The relative abundance of endophytic fungi in different sex *T. mairei* trees under UV-B radiation. **e** Venn analysis of the differential fungal genus in different sex *T. mairei* trees under UV-B radiation. **f** Proportion of common fungal genus in different sample groups

well separated at the genus level, indicating that exposure to UV-B radiation had a greater factor effect on differences among fungal communities than sex (Fig. 4c).

Based on the amplicon sequence variants (ASVs), all endophytic fungal species were assigned to 233 genera (Table S8). The relative abundance of all fungal species was analyzed at the genus level (Fig. 4d). In the F_0 h group, *Pestalotiopsis*, *Mycosphaerella*, and *Ascomycota* was the dominance fungal genus; in the M_0 h group, the dominance genus was *Ascomycota*, *Herpotrichiellaceae*, and *Glomerella*; in the F_48 h group, *Guignardia*, *Glomerella*, and *Herpotrichiellaceae* were the top three known dominance genus; and in the M_48 h group, *Glomerella*, *Herpotrichiellaceae*, and *Alternaria* were significantly enriched (Figure S5). Venn analysis identified 314 F_0 h specific genera, 318 M_0 h specific genera, 249 M_48 h specific genera, and 195 F_48 h specific genera. Interestingly, only 96 fungal genera were common among all four sample groups, suggesting that both sex and exposure to UV-B radiation significantly affected the fungal communities of *T. mairei* trees (Fig. 4e). Among the common fungal genera, *Glomerella* (15.45%), *Guignardia* (12.88%), *Herpotrichiellaceae* (9.44%), *Pestalotiopsis* (8.37%), and *Ascomycota* (8.37%) accounted for more than half of the total (Fig. 4f).

Exposure to UV-B radiation and sex influence the microbiome assemblies of *T. mairei*

The fungal communities of *T. mairei* were significantly affected by sex. To determine the effects of sex, the linear discriminant analysis effect size (LEfSe) analysis was used to identify biomarker taxa among the different sample groups. By the F/M_0 h comparison, the most significant fungal biomarker taxa in female trees were the genera *Pestalotiopsis*, *Alternaria*, *Rhizophydium*, *Hypocrea*, and *Candida*, and the most significant fungal biomarker taxa in male trees were the genera *Herpotrichiellaceae* and *Cyphellophora*. By the F/M_48 h comparison, the genus *Guignardia* was identified as a significant fungal biomarker taxon in female trees, while no significant fungal genus was identified as a biomarker taxon in male trees (Fig. 5a).

Plant endophytic fungal communities exhibit significant complexity. Changes to the abundances of 31 genus indicators among the different sample groups are shown in Figure S6. To simplify the complexity, three typical genus indicators, including *Guignardia*, *Alternaria*, and *Glomerella*, were selected for further analysis. In response to UV-B radiation, the abundance of *Guignardia* was significantly up-regulated in female trees and down-regulated in male trees, while the abundance of *Alternaria* showed opposite trends and the abundance of *Glomerella* remained relatively stable among the different sample groups (Fig. 5b). Sankey plot analysis also confirmed these changes to the relative abundance of the three typical genus indicators among the different sample groups (Fig. 5c). Meanwhile, correlation analysis showed a strong negative correlation between *Guignardia* and *Alternaria* (Rho = −0.46), but no significant correlation between *Guignardia-Glomerella* and *Alternaria-Glomerella* (Figure S7a).

Correlations between host gene expression and differential fungal taxa

Pearson correlation analysis was employed to identify potential correlations between the differential fungal genera and the host DEGs. *Guignardia* showed a positive correlation between the secondary metabolism-related DEGs and the expression levels of *APX2*, *GST7*, *ADT2*, *ZE1*, *ZE2*, *ZE4*, *NCED1*, and *NCED2*, and a negative correlation with the expression levels of *DHQS1*, *CM1*, and *CS1*. Meanwhile, *Alternaria* was positively correlated with the expression of *GST-Px1* and negatively correlated with the expression of *METTL17* (Fig. 5d). Among the TF-coding genes, both *Ascomycota* and *Chaetothyriales* were positively correlated with the expression of *ABR1*, *TEM1.2*, *MYB35*, *TEM1.1*, *SAP1*, and *RAV1*. Meanwhile, *Glomerella* and *Guignardia* were negatively correlated with the expression of *bZIP1* and *MADS1*, respectively (Figure S7b).

Functional prediction of the differential fungal taxa in *T. mairei*

The PICRUSt (Phylogenetic Investigation of Communities by Reconstruction of Unobserved States) algorithm was used to predict the potential function of the different fungal taxa in *T. mairei* (Table S9). The results showed that the dominant fungi in the F_0h group involved pathways related to geranylgeranyl diphosphate synthase- and *trans*-cinnamate 4-monooxygenase, while those of the F_48h group involved pathways related to quercetin 3-*O*-methyltransferase, peroxidase, and alpha-*L*-fructosidase, the only one of the M_0 h group involved the glutathione transferase-related pathway, and those of the M_48 h group involved pathways related to 2′-hydroxyisoflavone reductase and riboflavin kinase (Fig. 5e). Functional prediction suggested the involvement of sex-related differential endophytic fungi in the regulation of secondary metabolism in the host plant.

Isolation of endophytic fungi involved in sex-mediated responses to UV-B radiation

To investigate the function of endophytic fungi in sex-mediated responses to UV-B radiation, various endophytic fungal isolates were isolated from *T. mairei* (Fig. 6a). Based on morpho-taxonomy, the isolates were

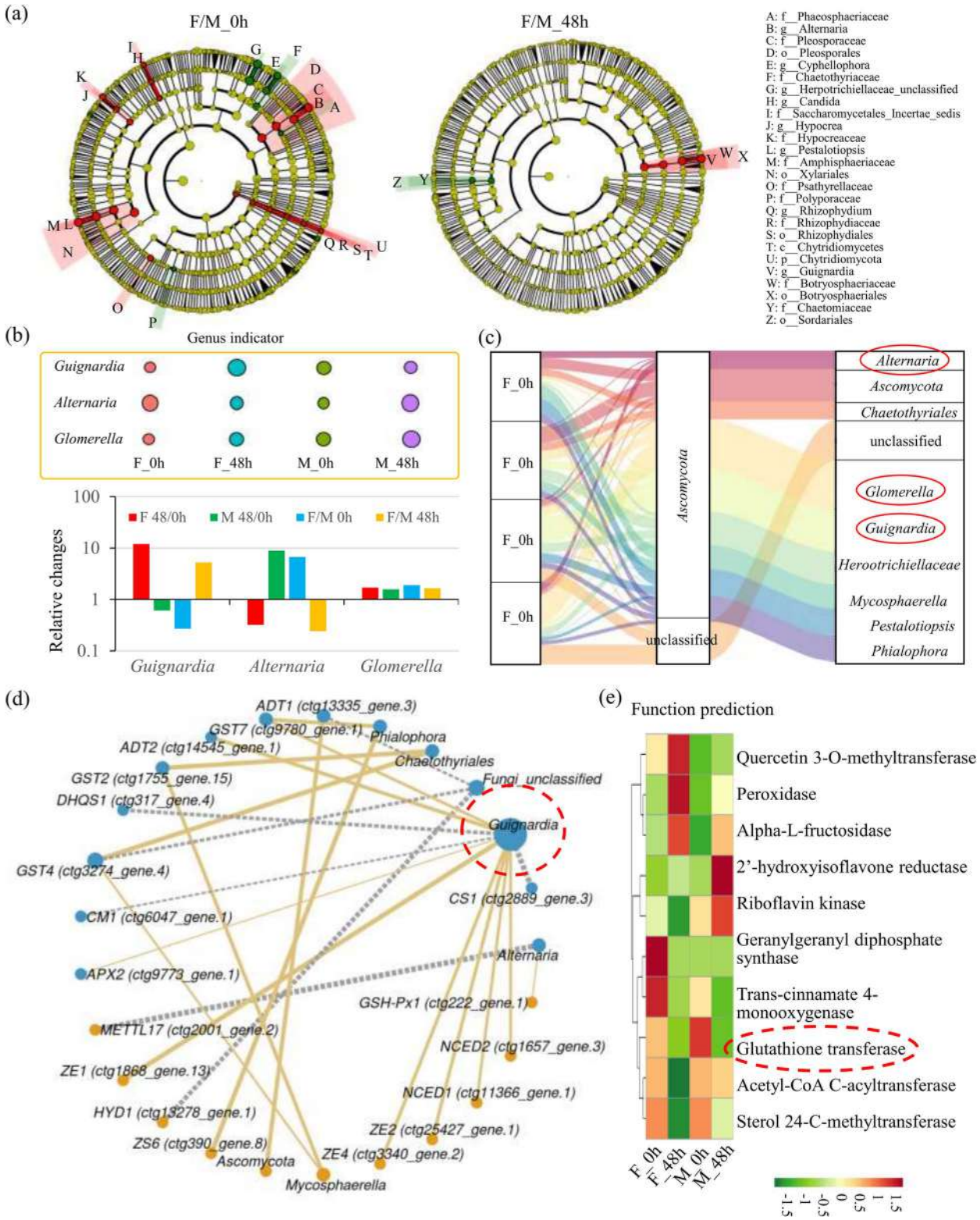

Fig. 5 UV-B radiation and sex affect the plant-microbiome assemblies of *T. mairei.* **a** Cladograms of Linear discriminant analysis coupled with the effect size analysis (LEfSe) analysis of the differences in abundant taxa of endophytic fungal between the female and male trees at the genus level. **b** Analysis of the differences in the abundance of three typic genus indicators in different sample groups. **c** Sankey plot of the changes in the relative abundance of the three typic genus indicators among different sample groups. **d** Pearson correlation analysis of differential fungal genus and host's DEGs. **e** Functional prediction of the three typic fungal genera using the PICRUSt2 program

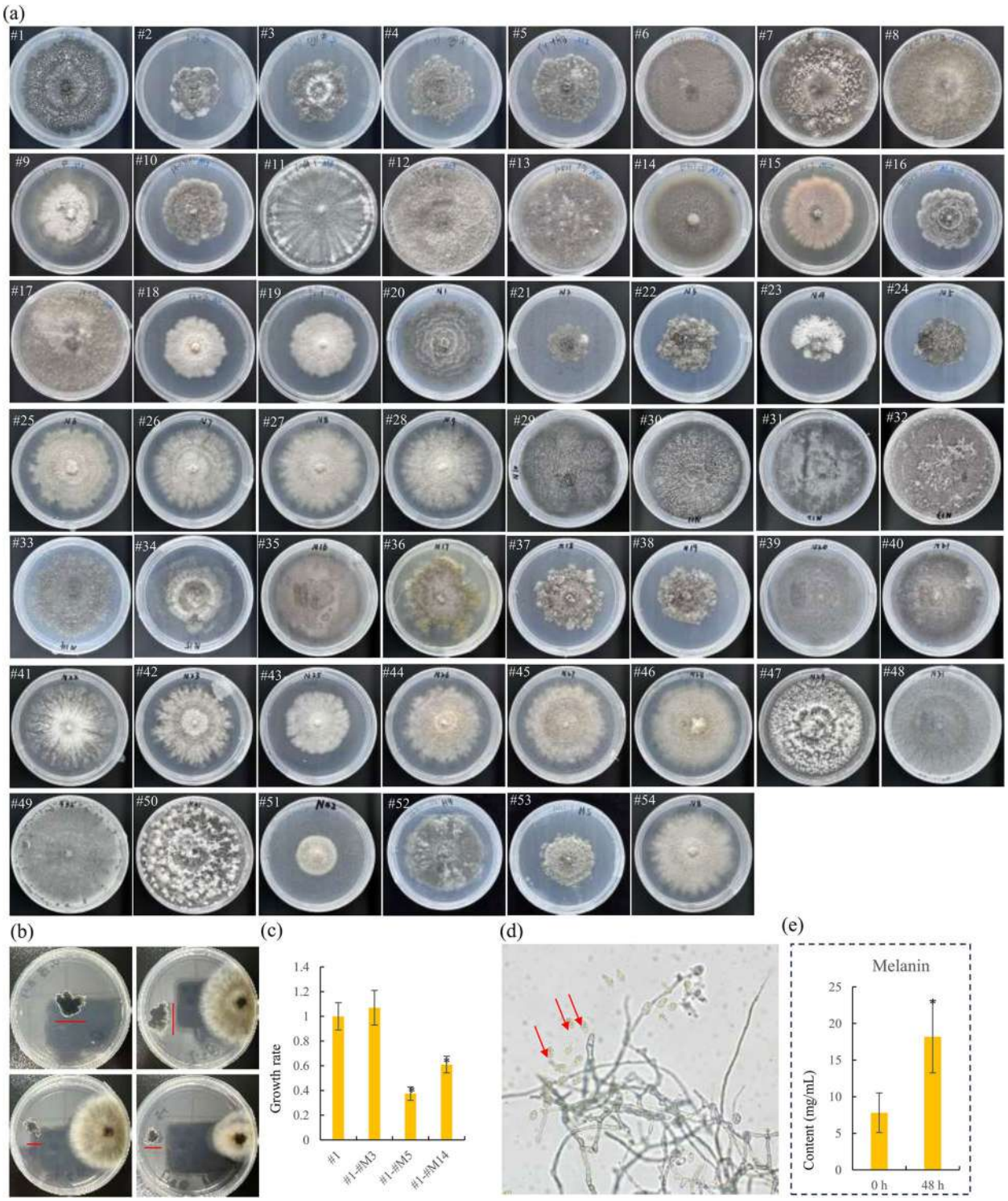

Fig. 6 Isolation of endophytic fungi involved in the sex-mediated responses to UV-B radiation. **a** The isolated endophytic fungal isolates were observed in plates. **b** The co-culture interactions between *Guignardia* isolate #1 and *Alternaria* #M3/M5/M14 on PDA. **c** Histogram showed the growth rate of *Guignardia* isolates #1 under different conditions. **d** A picture of *Guignardia* isolate #1 from *T. mairei*. Red arrows indicated spores from *Guignardia* isolate #1. **e** The melanin content in *Guignardia* isolate #1 under control and UV-B radiation conditions. "*" indicated the significance value $P < 0.01$

assigned to the genera *Alternaria*, *Chaetomium*, *Cladosporium*, *Colletotrichum*, *Didymella*, *Guignardia*, *Lentithecium*, *Muyocopron*, *Nigrospora*, *Paraconiothyrium*, *Perenniporia*, *Pezicula*, *Phyllosticta*, *Stilbohypoxylon*, and *Trichoderma* (Table S10). Fortunately, one *Guignardia* isolate (#1) and three *Alternaria* isolates (#7, #8, and #17) were identified, providing an opportunity to reveal the roles of endophytic fungi in sex-mediated responses to UV-B radiation (Figure S8).

To confirm the negative correlation between *Guignardia* and *Alternaria*, the antagonistic activities of three *Alternaria* isolates against *Guignardia* were determined using co-culture assays (Fig. 6b). The endophytic fungal isolates #8 and #17 inhibited the growth of *Guignardia* isolate #1 by 62.6% and 39.0%, respectively. *Alternaria* isolate #7 did not inhibit growth of the *Guignardia* isolate #1 (Fig. 6c). *Guignardia* is a spore-producing fungus (Fig. 6d). It is worth mentioning that *Guignardia* isolate #1 had a high melanin content of 7.8 mg/mL, which was increased to 18.2 mg/mL by exposure to UV-B radiation (Fig. 6e).

Effect of inoculation with *Guignardia* spores on host gene expression

Considering the complexity of the interactions between endophytic fungi and hosts, the key spore-producing *Guignardia* isolate #1 was selected for inoculation assays. *Guignardia* isolate #1 was incubated on PDA for 7 days, which produced a large number of spores. Then, the concentration of *Guignardia* isolate #1 spores was adjusted to 1×10^6/mL for artificial infection. After 48 h of incubation with spores produced by *Guignardia* isolate #1, twigs of female *T. mairei* were harvested for RNA-seq (Fig. 7a).

The correlation between the two samples was calculated and shown in a correlation heatmap, which confirmed the reliability of the experiments (Figure S9a). The percentages of the explained values of PC1 and PC2 were 85.34% and 7.74%, respectively, suggesting dramatic differences among the different sample groups (Figure S9b). Among the 2330 screened DEGs, 801 were up-regulated and 1529 were down-regulated after infection with spores produced by *Guignardia* isolate #1 (Fig. 7b and Table S11). Most of the DEGs responsive to infection with spores produced by *Guignardia* isolate #1 were associated with at least one GO term (Fig. 9Sc). The significantly enriched GO terms in response to UV-B radiation and taxol biosynthesis were "cellular response to light stimulus", "response to light stimulus", "response to high light intensity", "photosystem I", and "photosystem II" (Fig. 7c). Infection with spores produced by *Guignardia* isolate #1 greatly activated responses to light stress. KEGG enrichment analysis identified several metabolism-related pathways that were significantly altered by infection of spores produced by Guignardia isolate #1, which included "cyanoamino acid metabolism" ($P=3.16E-10$), "glyoxylate and dicarboxylate metabolism" ($P=3.41E-06$), "flavonoid biosynthesis" ($P=0.0037$), and "glutathione metabolism" ($P=2.95E-05$) (Figure S10).

Hence, further analysis was conducted to investigate the expression patterns of *Guignardia*-correlated UV-B-responsive genes. The results showed that infection with spores produced by *Guignardia* isolate #1 significantly increased expression of two genes related to glutathione metabolism (*APX2* and *GST7*), two related to carotenoid biosynthesis (*NCED1* and *ZE1*), and two related to phenylalanine and tyrosine biosynthesis (*CM1* and *CS1*) (Fig. 7d). The key DEGs were confirmed by qRT-PCR experiment (Figure S11).

Effect of inoculation with spores produced by *Guignardia* on metabolite accumulation in the host

Untargeted metabolomics was applied to determine the effect of *Guignardia* inoculation on metabolite accumulation in the host. Based on annotation information, an enormous number of potential metabolites were predicted, including 2146 lipids, 877 organoheterocyclic compounds, 803 phenylpropanoids, and 745 organic acids, etc. (Figure S12a). Metabolite profiling showed great variations in the metabolomes of *T. mairei* after infection with spores produced by *Guignardia* isolate #1. PCA showed that the PC1 and PC2 values were 62.7% and 5.32%, respectively (Figure S12b). Statistical analysis identified 655 differentially accumulated metabolites (DAMs), including 322 up- and 333 downregulated metabolites (Figure S12c).

Three metabolites related to carotenoid biosynthesis were detected, among which 9,9″-di-cis-ζ-carotene and pre-squalene diphosphate were significantly up-regulated by infection with spores produced by *Guignardia* isolate #1. Of the three metabolites related to the biosynthesis of phenylalanine and tyrosine, L-tryptophan and L-phenylalanine were significantly up-regulated by infection with spores produced by *Guignardia* isolate #1. Of two metabolites related to glutathione metabolism, glutathione was significantly up-regulated by infection with spores produced by *Guignardia* isolate #1. Interestingly, infection with spores produced by *Guignardia* isolate #1 was associated with increased melatonin content (Fig. 7e).

Discussion

Prior related studies mostly concentrated on UV-B radiation as an essential regulator of many physiological processes in plants, such as secondary metabolism [35]. Enhanced UV-B radiation was reported to have various

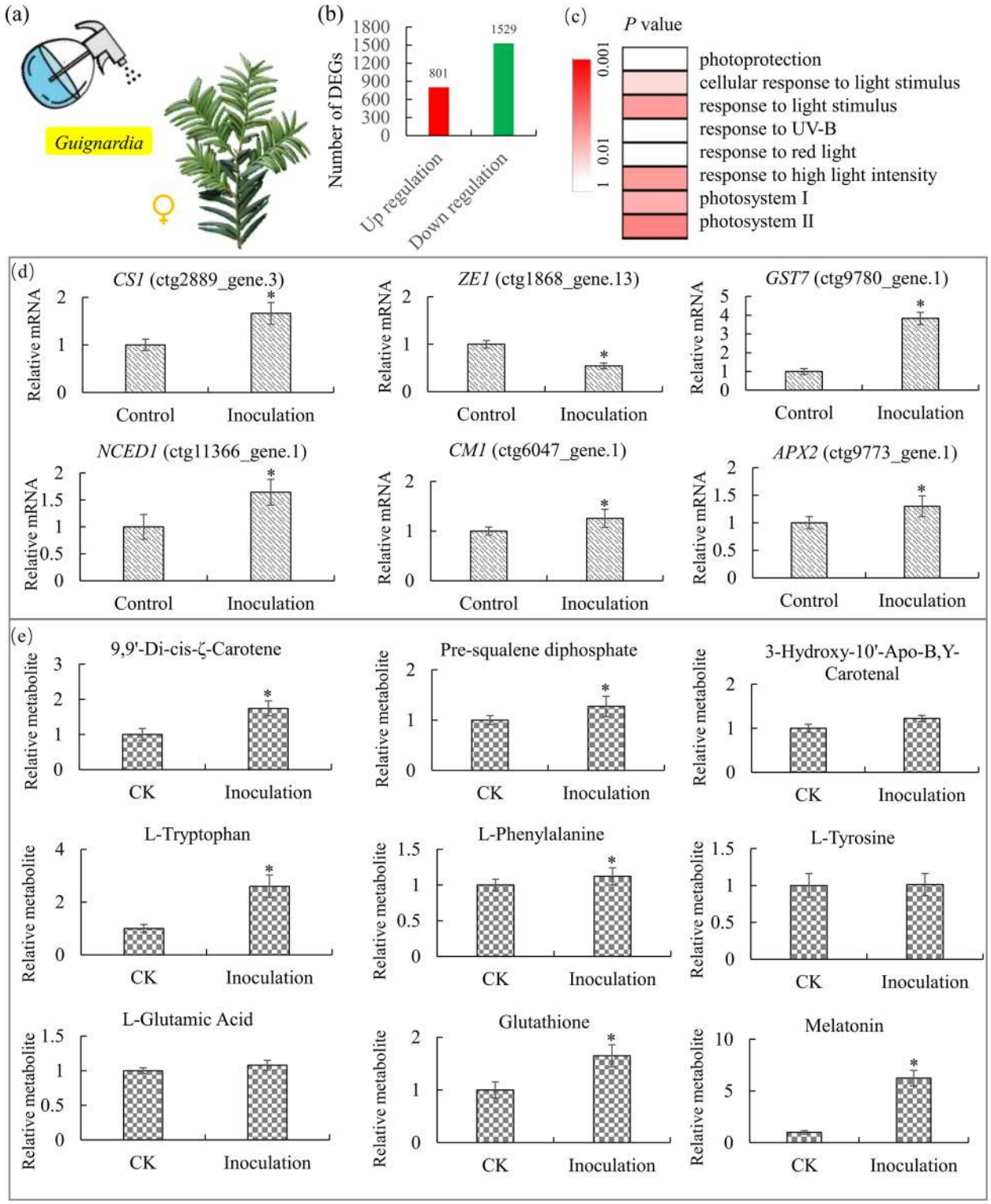

Fig. 7 Effect of inoculation with *Guignardia* on the host's gene expression and metabolite accumulation. **a** The spores of *Guignardia* isolate #1 were sprayed onto the twigs of female *T. mairei*. **b** The number of up-regulated and down-regulated genes after *Guignardia* isolates #1 spore infection. **c** Enrichment analysis of the light-responsive GO terms. **d** Expression analysis of *Guignardia*-correlated UV-B responsive genes. "*" indicated the significance value $P < 0.01$. **e** Accumulation analysis of several key metabolites. "*" indicated the significance value $P < 0.01$

negative effects on the development and growth of plants [36]. More recent studies have focused on how plants adapt and utilize UV-B radiation.

The roles of sex in the morphological and physiological responses of dioecious plants to UV-B radiation have been deeply studied. As compared to females, male *P. cathayana* have a more efficient antioxidant system to alleviate stress induced by exposure to UV-B radiation [37]. In *Salix myrsinifolia*, males have thinner leaves and are less tolerant to UV-B radiation than females [38]. In *P. tremula*, males are more responsive to increased UV-B radiation than females [39]. Although the morphologic, physiologic, and biochemical responses of *Taxus* to UV-B radiation have been well studied, the effect of sex on the responses of *T. mairei* to UV-B radiation remains largely unknown [21, 28].

High-throughput sequencing has provided strong evidence of sex-biased gene expression in dioecious plants [5]. In *T. mairei*, several GO terms related to light-stimulated response were significantly enriched in female trees, suggesting a stronger transcriptional response of female trees to UV-B radiation than male trees. Stress caused by exposure to UV-B radiation can inhibit photosynthesis [40]. In the present study, more photosynthesis-related DEGs were identified in female trees, suggesting a greater effect of UV-B radiation on energy supply than female trees. Long-term exposure of plants to UV-B radiation results in the accumulation of reactive oxygen species (ROS), such as hydrogen peroxide, superoxide anion radicals, and hydroxyl ions [41]. During the evolutionary process, plants have developed efficient systems to protect against damage from exposure to UV-B radiation, which consists of various types of secondary metabolites, such as flavonoids and carotenoids, as well as a variety of antioxidants, such as ascorbate and glutathione [42]. Activation of phenylalanine ammonia-lyase and tyrosine aminotransferase can alleviate damage caused by UV-B stress [43]. Glutathione-mediated antioxidant processes are enhanced in plants to protect against UV-B stress [44]. UV-B-induced carotenoid production can protect the photosynthetic machinery from damage induced by UV-B radiation [45]. In response to UV-B radiation, sex significantly influenced the expression of *T. mairei* genes related to "flavonoid biosynthesis", "flavone and flavonol biosynthesis", "glutathione metabolism", "carotenoid biosynthesis", and "brassinosteroid biosynthesis". The results of this study also showed that sex influences the efficient removal of ROS produced in response to UV-B radiation by regulating pathways related to the metabolism of amino acids, glutathione, and carotenoids.

Previous studies reported notable differences in morphology, physiology, and gene expression profiles between female and male *Taxus* trees under normal growth conditions. For example, sex differences in the C:N ratio and increment biomass were observed in *T. baccata* trees [46]. A recent study revealed sex-dependent variation of leaf traits along altitude gradients in the *T. fuana* population [47]. In *T. media*, female trees contained higher amounts of taxoids than male trees [34]. Although a large number of DEGs were identified, expression of the sex-related DEGs was significantly influenced by exposure to UV-B radiation. However, only 166 common DEGs were detected, suggesting that UV-B radiation greatly altered sexual dimorphism.

Effects of UV-B radiation on the diversity and activity of microbial communities have been extensively studied [48, 49]. In *T. mairei*, alpha and beta diversity analysis indicated that the relative abundances of dominant fungi and indicator genera changed considerably. In addition to environmental factors, plant sex affects microbial communities of dioecious trees [8]. Although the effects of UV-B radiation on endophytic fungal communities were stronger than sex, a number of sex-related differential endophytic fungi were identified in *T. mairei*. Under control conditions, fungal genera *Cyphellophora*, *Herpotrichiellaceae*, *Rhizophydium*, *Candida*, *Alternaria*, *Pestalotiopsis*, and *Hypocrea* were significantly altered by sex, suggesting the presence of sex-dependent functions in *T. mairei* endophytes. The deterministic filtration process of plant microbiota is dependent on the host metabolites, phytohormones, and innate immune system [50]. Transcriptomic analysis revealed the effects of sex on various secondary metabolic pathways, which provide chemical resources for the host to produce attractants and/or inhibitors to filter microbial taxa [51]. Notably, *Guignardia* was the only genus of endophytic fungi significantly influenced by the sex of *T. mairei* in response to UV-B radiation, suggesting that UV-B radiation greatly reduced sex-mediated filtration of microbiota. In *Populus* species, environmental stressors might cause larger alterations to plant microbiota and increase the differences in populations of endophytic fungi between female and male trees [3, 8, 51]. However, stress caused by UV-B radiation significantly reduced the effect of sex on fungal communities, indicating that *Taxus* has a different sex regulation mechanism than *Populus* in response to environmental stress.

Isolation of key endophytic fungi is an effective method to investigate the roles of endophytes in sex-related responses of *T. mairei* to UV-B radiation. In the present study, a large number of endophytic fungal isolates were isolated, providing sufficient research materials. Correlation analysis was focused on one *Guignardia* isolate (#1) and three *Alternaria* isolates (#7, #8, and #17). In *Taxus*, *Guignardia* and *Alternaria* are two common genera of endophytic fungi

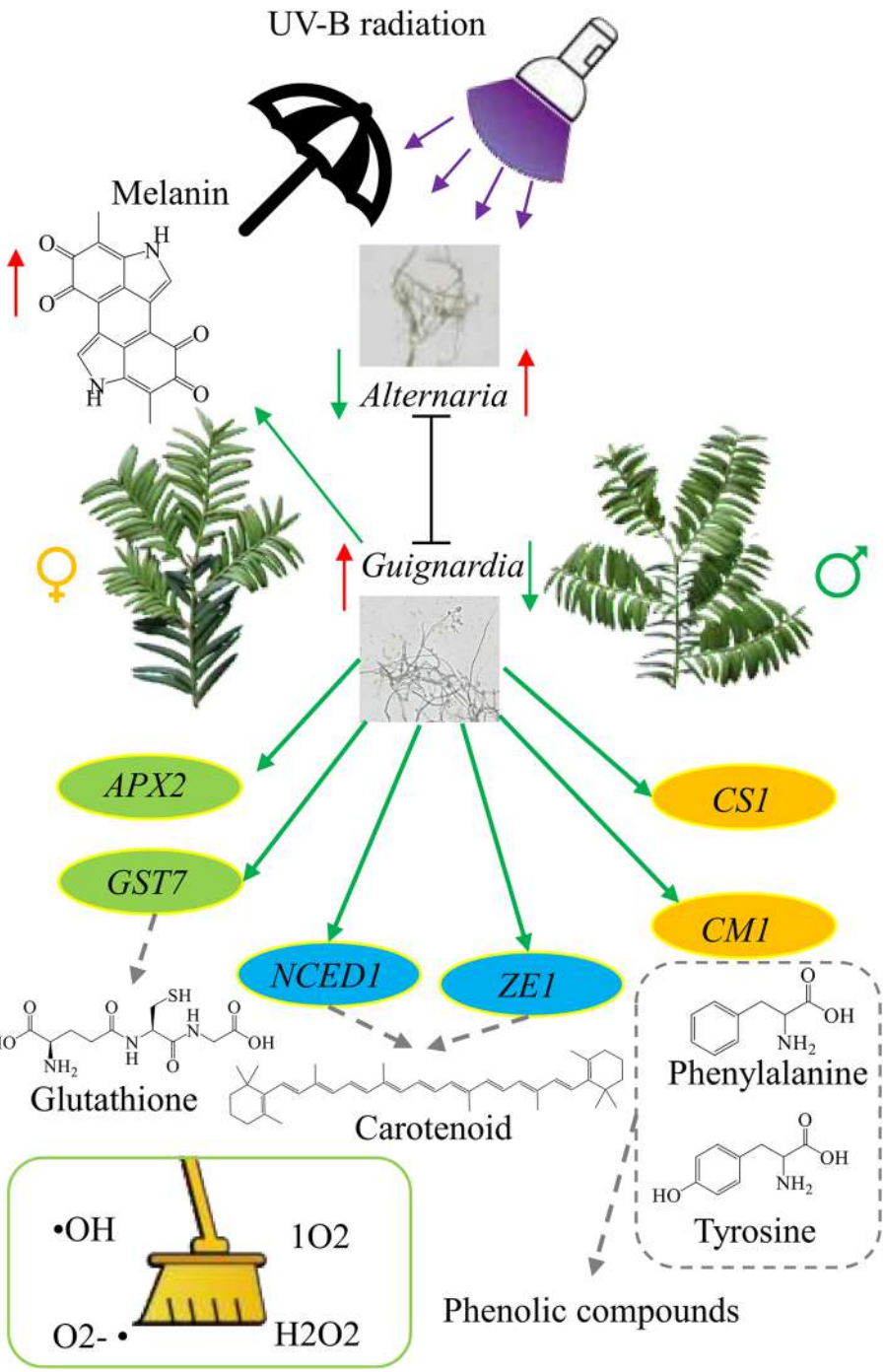

Fig. 8 A hypothetical model for the regulatory mechanism involved in sex-mediated responses to UV-B radiation. *Guignardia* isolate #1 inoculation significantly altered various oxidation–reduction systems, such as glutathione metabolism and carotenoid biosynthesis pathway, by regulating the expression of *APX2*, *GST7*, *NCED1*, *ZE1*, *CS1*, and *CM1*

known for potential taxol production [52–54]. However, relatively few studies have investigated the roles of *Guignardia* and *Alternaria* in host responses to UV-B radiation. Melanin in the hyphae of *Guignardia mangiferae*, a common endophyte of woody trees, is believed to be responsible for the ability of fungi to survive in stressful environments [55]. *Guignardia* isolate #1 had a relatively high content of melanin, which might have been significantly induced by UV-B radiation. Enhanced production of melanin improved

the survival ability of *Guignardia* isolate #1 in female trees in response to UV-B radiation and significantly altered the fungal community structure through fungal interactions. The antagonistic relationship between *Guignardia* isolate #1 and *Alternaria* isolates #8 and #17 supports this assumption. The variation in internal chemical microenvironments may be the primary factor contributing to the differentiation of endophytic fungi between female and male trees exposed to UV-B radiation [56].

Endophytic fungi also promote development, enhance antioxidant defense systems, and induce the accumulation of secondary metabolites in the host plant [57]. For example, inoculation with several specific fungal endophytes promoted the total flavonoid and phenolic contents in grape cells [58]. In a previous study, various endophytic fungi with growth- and metabolism-promoting capabilities and potential economic benefits were isolated from the different tissues of *Taxus* [52]. In the present study, inoculation of spores produced by *Guignardia* isolate #1 significantly altered the photosynthesis and oxidation–reduction systems of *T. mairei*, which simulated the responses of plants to UV-B radiation and also activated the glutathione metabolism and carotenoid biosynthesis pathways, which increased production of antioxidants. The enzymes glutathione S-transferase and ascorbate peroxidase are reportedly involved in the interactions of the host plant with fungal pathogens [59]. Integrated transcriptomic and metabolomic analyses indicated that *Guignardia* inoculation enhanced the glutathione content by up-regulating expression of *APX2* and *GST7*. Phenolic compounds and carotenoids are bioactive compounds with high antioxidant capacities, which play important roles in removing accumulated free radicals [60]. *Guignardia* inoculation significantly elevated production of carotenoids and the precursors of phenolic acids by altering the expression profiles of *NCED1*, *ZE1*, *CS1*, and *CM1* (Fig. 8). Interestingly, inoculation of *Guignardia* enhanced the melanin content, indicating that fungal symbiosis contributed to the maintenance of endogenous melanin biosynthesis in *T. mairei*.

Conclusions

Our results provided strong evidence that sex affects the efficiency of removing accumulated ROS induced by UV-B radiation by regulating pathways associated with the metabolism of amino acids, glutathione, and carotenoids. ITS-seq analysis identified various differential endophytic fungi between female and male *T. mairei* trees. Sex affects various secondary metabolic pathways, providing a chemical base for *T. mairei* host to produce attractants and/or inhibitors to filter microbial taxa. Furthermore, correlation analysis and biomarker screening focused on a sex-related endophyte, specifically *Guignardia* isolate #1, which significantly altered various oxidation–reduction systems, such as glutathione metabolism and the carotenoid biosynthesis pathway, by regulating the expression of *APX2*, *GST7*, *NCED1*, *ZE1*, *CS1*, and *CM1*. Overall, further investigations of the effects of endophytic fungi on sex-mediated responses to UV-B radiation will be helpful in providing valuable insights into how dioecious trees respond to environmental stress in a sex-specific manner.

Supplementary Information

The online version contains supplementary material available at https://doi.org/10.1186/s40168-024-01882-1.

Supplementary Material 1: Table S1. All the primer sequences for qRT-PCR.

Supplementary Material 2: Table S2. The detail information of the RNA-seq samples.

Supplementary Material 3: Table S3. The detail information of the RNA-seq reads mapping onto the *T. mairei*.

Supplementary Material 4: Table S4. The detail information of the tags from ITS-seq.

Supplementary Material 5: Table S5. The UV-B responsive genes in female trees.

Supplementary Material 6: Table S6. The UV-B responsive genes in male tree.

Supplementary Material 7: Table S7. Differentially expressed TFs between the female and male trees.

Supplementary Material 8: Table S8. The information of 233 endophytic fungal genus based on the ASV sequences.

Supplementary Material 9: Table S9. Prediction of potential function of the differential fungal taxa in *T. mairei*.

Supplementary Material 10: Table S10. The detail information of endophytic fungal isolates from *T. mairei*.

Supplementary Material 11: Table S11. The DEGs treated by *Guignardia* isolate #1.

Supplementary Material 12: Figure S1. The correlation value between each comparison of two RNA-seq samples.

Supplementary Material 13: Figure S2. Expression analysis of the DEGs under UV-B radiation.

Supplementary Material 14: Figure S3. GO enrichment analysis of the DEGs responsive to UV-B radiation.

Supplementary Material 15: Figure S4. Alpha and beta diversity analysis of fungal communities under UV-B radiation in *T. mairei* trees.

Supplementary Material 16: Figure S5. The relative abundance of all fungal in different sample groups.

Supplementary Material 17: Figure S6. Analysis of the differences in abundance of 31genus indicators in different sample groups.

Supplementary Material 18: Figure S7. Relations between host gene expression and differential fungal taxa.

Supplementary Material 19: Figure S8. ITS identification of #1, #7, #8, and #17 fungal isolates.

Supplementary Material 20: Figure S9. Overview of the transcriptomic analysis of the DEGs under *Guignardia* isolate #1 infection.

Supplementary Material 21: Figure S10. KEGG enrichment analysis of the DEGs responsive to *Guignardia* isolate #1 spore infection.

Supplementary Material 22: Figure S11. Real-time PCR validation.

Supplementary Material 23: Figure S12. Metabolite profiling of *T. mairei* after *Guignardia* isolate #1 spore infection.

Acknowledgements
We are grateful to LC Sciences Company (Hangzhou, China) and OEbiotech Co., Ltd (Shanghai, China) for transcriptomic and metabolomic analysis, respectively.

Authors' contributions
H.Z., H.W. and C.S. conceptualized the initial study; H.Z., H.K., Q.Y. and C.S. were involved in the design of experiments; H.Z., H.K., X.L., W.L., R.M., Y.Z., X.Z. and M.W. performed the lab experiments; H.Z., S.F., B.Z. and C.S. drafted the initial article.

Funding
This work was funded by the National Natural Science Foundation of China (32271905 and 32270382), the Zhejiang Provincial Natural Science Foundation of China (Grant Nos. LY23C160001, LY18C050005, LY19C150005, and LY19C160001). Opening Project of Zhejiang Provincial Key Laboratory of Forest Aromatic Plants-based Healthcare Functions (2022E10008).

Availability of data and materials
The raw transcriptome sequencing data are uploaded to the National Center for Biotechnology Information under BioProject ID: PRJNA1025358. The raw ITS sequencing data are uploaded to the National Center for Biotechnology Information under BioProject ID: PRJNA1023917. The *T. mairei* reference genome was downloaded from the NCBI database (ID: PRJNA730337).

Declarations

Ethics approval and consent to participate
Not applicable.

Consent for publication
Not applicable.

Competing interests
The authors declare no competing interests.

Received: 9 November 2023 Accepted: 27 July 2024
Published online: 07 September 2024

References

1. Diggle PK, Di Stilio VS, Gschwend AR, Golenberg EM, Moore RC, Russell JR, Sinclair JP. Multiple developmental processes underlie sex differentiation in angiosperms. Trends Genet. 2011;27(9):368–76.
2. Liao Q, Du R, Gou J, Guo L, Shen H, Liu H, Nguyen JK, Ming R, Yin T, Huang S, et al. The genomic architecture of the sex-determining region and sex-related metabolic variation in *Ginkgobiloba*. Plant J. 2020;104(5):1399–409.
3. Duan D, Jia Y, Yang J, Li ZH. Comparative transcriptome analysis of male and female conelets and development of microsatellite markers in *Pinus bungeana*, an Endemic Conifer in China. Genes (Basel). 2017;8(12):393.
4. Wu X, Liu J, Meng Q, Fang S, Kang J, Guo Q. Differences in carbon and nitrogen metabolism between male and female *Populus cathayana* in response to deficient nitrogen. Tree Physiol. 2021;41(1):119–33.
5. Han Q, Song H, Yang Y, Jiang H, Zhang S. Transcriptional profiling reveals mechanisms of sexually dimorphic responses of Populus cathayana to potassium deficiency. Physiol Plant. 2018;162(3):301–15.
6. Keefover-Ring K, Carlson CH, Hyden B, Azeem M, Smart LB. Genetic mapping of sexually dimorphic volatile and non-volatile floral secondary chemistry of a dioecious willow. J Exp Bot. 2022;73(18):6352–66.
7. He F, Wu Z, Zhao Z, Chen G, Wang X, Cui X, Zhu T, Chen L, Yang P, Bi L, et al. Drought stress drives sex-specific differences in plant resistance against herbivores between male and female poplars through changes in transcriptional and metabolic profiles. Sci Total Environ. 2022;845:157171.
8. Guo Q, Liu L, Liu J, Korpelainen H, Li C. Plant sex affects plant-microbiome assemblies of dioecious *Populus cathayana* trees under different soil nitrogen conditions. Microbiome. 2022;10(1):191.
9. Guo Q, Liu J, Yu L, Korpelainen H, Li C. Different sexual impacts of dioecious *Populus euphratica* on microbial communities and nitrogen cycle processes in natural forests. For Ecol Manage. 2021;496:119403.
10 Zhou Y, Pang Z, Yuan Z, Fallah N, Jia H, Ming R. Sex-based metabolic and microbiota differences in roots and rhizosphere soils of dioecious papaya (Carica papaya L.). Front Plant Sci. 2022;13:991114.
11. Liu L, Lu L, Li H, Meng Z, Dong T, Peng C, Xu X. Divergence of phyllosphere microbial communities between females and males of the dioecious *Populus cathayana*. Mol Plant Microbe Interact. 2021;34(4):351–61.
12. Xia Z, He Y, Yu L, Li Z, Korpelainen H, Li C. Revealing interactions between root phenolic metabolomes and rhizosphere bacterial communities in Populus euphratica plantations. Biol Fertil Soils. 2021;57:421–34.
13. Xia Z, He Y, Yu L, Lv R, Korpelainen H, Li C. Sex-specific strategies of phosphorus (P) acquisition in *Populus cathayana* as affected by soil P availability and distribution. New Phytol. 2020;225(2):782–92.
14. Feng S, Kailin H, Zhang H, Chen C, Huang J, Wu Q, Zhang Z, Gao Y, Wu X, Wang H, et al. Investigation of the role of TmMYB16/123 and their targets (TmMTP1/11) in the tolerance of Taxus media to cadmium. Tree Physiol. 2023;43(6):1009–22.
15. Liu J, Zhang R, Xu X, Fowler JC, Miller TEX, Dong T. Effect of summer warming on growth, photosynthesis and water status in female and male Populus cathayana: implications for sex-specific drought and heat tolerances. Tree Physiol. 2020;40(9):1178–91.
16. Zhao H, Xu X, Zhang Y, Korpelainen H, Li C. Nitrogen deposition limits photosynthetic response to elevated CO2 differentially in a dioecious species. Oecologia. 2011;165(1):41–54.
17. Diaz-Barradas MC, Zunzunegui M, Correia O, Ain-Lhout F, Esquivias MP, Alvarez-Cansino L. Gender dimorphism in Corema album across its biogeographical area and implications under a scenario of extreme drought events. Environ Exp Botany. 2018;155:10.
18. Lin T, Tang J, Li S, Li S, Han S, Liu Y, Yang C, Chen G, Chen L, Zhu T. Drought stress mediated differences in phyllosphere microbiome and associated pathogen resistance between male and female poplars. Plant J. 2023;115(4):1100–13.
19. Kreft I, Vollmannova A, Lidikova J, Musilova J, Germ M, Golob A, Vombergar B, Kocjan Acko D, Luthar Z. Molecular shield for protection of buckwheat plants from UV-B Radiation. Molecules. 2022;27(17):5577.
20. Li Y, Qin W, Fu X, Zhang Y, Hassani D, Kayani SI, Xie L, Liu H, Chen T, Yan X, et al. Transcriptomic analysis reveals the parallel transcriptional regulation of UV-B-induced artemisinin and flavonoid accumulation in Artemisia annua L. Plant Physiol Biochem. 2021;163:189–200.
21 Jiao J, Xu XJ, Lu Y, Liu J, Fu YJ, Fu JX, Gai QY. Identification of genes associated with biosynthesis of bioactive flavonoids and taxoids in Taxus cuspidata Sieb. et Zucc. plantlets exposed to UV-B radiation. Gene. 2022;823:146384.
22. Yu C, Hou K, Zhang H, Liang X, Chen C, Wang Z, Wu Q, Chen G, He J, Bai E, et al. Integrated mass spectrometry imaging and single-cell transcriptome atlas strategies provide novel insights into taxoid biosynthesis and transport in Taxus mairei stems. Plant J. 2023;115(5):1243–60.
23. Zhan X, Qiu T, Zhang H, Kailin H, Liang X, Chen C, Wang Z, Wu Q, Wang X, Li XL, et al. Mass spectrometry imaging and single-cell transcriptional profiling reveal the tissue-specific regulation of bioactive ingredient biosynthesis in Taxus leaves. Plant Commun. 2023;4(5):100630.
24. Xu H, Li Y, Guo J, Sui Y, Chen B, Li D, Jiang J. A meta-analysis of the efficacy of albumin paclitaxel versus docetaxel in the treatment of breast cancer. J Healthc Eng. 2021;2021:7020177.
25. Perez-Matas E, Hidalgo-Martinez D, Escrich A, Alcalde MA, Moyano E, Bonfill M, Palazon J. Genetic approaches in improving biotechnological production of taxanes: an update. Front Plant Sci. 2023;14:1100228.
26. Xu M, Shen C, Zhu Q, Xu Y, Xue C, Zhu B, Hu J. Comparative metabolomic and transcriptomic analyses revealed the differential accumulation of secondary metabolites during the ripening process of acerola cherry (Malpighia emarginata) fruit. J Sci Food Agr. 2022;102(4):1488–97.
27. Yu C, Luo X, Zhang C, Xu X, Huang J, Chen Y, Feng S, Zhan X, Zhang L, Yuan H, et al. Tissue-specific study across the stem of Taxus media identifies a phloem-specific TmMYB3 involved in the transcriptional regulation of paclitaxel biosynthesis. Plant J. 2020;103(1):95–110.

28. Zu YG, Pang HH, Yu JH, Li DW, Wei XX, Gao YX, Tong L. Responses in the morphology, physiology and biochemistry of Taxus chinensis var. mairei grown under supplementary UV-B radiation. J Photochem Photobiol B. 2010;98(2):152–8.
29. Tian Y, Amand S, Buisson D, Kunz C, Hachette F, Dupont J, Nay B, Prado S. The fungal leaf endophyte Paraconiothyrium variabile specifically metabolizes the host-plant metabolome for its own benefit. Phytochemistry. 2014;108:95–101.
30. Xu W, Bi H, Peng H, Yang L, He H, Fu G, Liu Y, Wan Y. Fermentative production of diacylglycerol by endophytic fungi screened from Taxus chinensis var. mairei. Foods. 2023;12(2):399.
31. Velez H, Gauchan DP, Garcia-Gil MDR. Taxol and beta-tubulins from endophytic fungi isolated from the Himalayan Yew. Taxus wallichiana Zucc Front Microbiol. 2022;13:956855.
32. Xiong X, Gou J, Liao Q, Li Y, Zhou Q, Bi G, Li C, Du R, Wang X, Sun T, et al. The Taxus genome provides insights into paclitaxel biosynthesis. Nat Plants. 2021;7(8):1026–36.
33. Douglas GM, Maffei VJ, Zaneveld JR, Yurgel SN, Brown JR, Taylor CM, Huttenhower C, Langille MGI. PICRUSt2 for prediction of metagenome functions. Nat Biotechnol. 2020;38(6):685–8.
34. Yu C, Huang J, Wu Q, Zhang C, Li XL, Xu X, Feng S, Zhan X, Chen Z, Wang H, et al. Role of female-predominant MYB39-bHLH13 complex in sexually dimorphic accumulation of taxol in *Taxus media*. Hortic Res. 2022;9:uhac062.
35. Narra F, Castagna A, Palai G, Havlik J, Bergo AM, D'Onofrio C, Ranieri A, Santin M. Postharvest UV-B exposure drives changes in primary metabolism, phenolic concentration, and volatilome profile in berries of different grape (Vitis vinifera L.) varieties. Plant Physiol Bioch. 2018;126:55–62.
36. Jansen MA, Bornman JF. UV-B radiation: from generic stressor to specific regulator. Physiol Plant. 2012;145(4):501–4.
37. Xu X, Zhao H, Zhang X, Hanninen H, Korpelainen H, Li C. Different growth sensitivity to enhanced UV-B radiation between male and female Populus cathayana. Tree Physiol. 2010;30(12):1489–98.
38 Ruuhola T, Nybakken L, Randriamanana T, Lavola A, Julkunen-Tiitto R. Effects of long-term UV-exposure and plant sex on the leaf phenoloxidase activities and phenolic concentrations of Salix myrsinifolia (Salisb.). Plant Physiol Bioch. 2018;126:55–62.
39. Stromme CB, Julkunen-Tiitto R, Krishna U, Lavola A, Olsen JE, Nybakken L. UV-B and temperature enhancement affect spring and autumn phenology in Populus tremula. Plant Cell Environ. 2015;38(5):867–77.
40. Liu M, Sun Q, Cao K, Xu H, Zhou X. Acetylated proteomics of UV-B stress-responsive in photosystem II of *Rhododendron chrysanthum*. Cells. 2023;12(3):478.
41. Tan Y, Duan Y, Chi Q, Wang R, Yin Y, Cui D, Li S, Wang A, Ma R, Li B, et al. The role of reactive oxygen species in plant response to radiation. Int J Mol Sci. 2023;24(4):3346.
42. Agati G, Brunetti C, Di Ferdinando M, Ferrini F, Pollastri S, Tattini M. Functional roles of flavonoids in photoprotection: new evidence, lessons from the past. Plant Physiol Biochem. 2013;72:35–45.
43. Zhao Z, Yun C, Gu L, Liu J, Yao L, Wang W, Wang H. Melatonin enhances biomass, phenolic accumulation, and bioactivities of rosemary (*Rosmarinus officinalis*) in vitro shoots under UV-B stress. Physiol Plant. 2023;175:e13956.
44. Ozgur R, Uzilday B, Yalcinkaya T, Akyol TY, Yildirim H, Turkan I. Differential responses of the scavenging systems for reactive oxygen species (ROS) and reactive carbonyl species (RCS) to UV-B irradiation in Arabidopsis thaliana and its high altitude perennial relative *Arabis alpina*. Photochem Photobiol Sci. 2021;20(7):889–901.
45. Badmus UO, Crestani G, Cunningham N, Havaux M, Urban O, Jansen MAK. UV radiation induces specific changes in the carotenoid profile of *Arabidopsis thaliana*. Biomolecules. 2022;12(12):1879.
46. Rabska M, Giertych MJ, Nowak K, Pers-Kamczyc E, Iszkulo G. Consequences of the reproductive effort of dioecious Taxus baccata L. females in a generative bud removal experiment-important role of nitrogen in female reproduction. Int J Mol Sci. 2022;23(22):14225.
47. Li TX, Shen-Tu XL, Xu L, Zhang WJ, Duan JP, Song YB, Dong M. Intraspecific and sex-dependent variation of leaf traits along altitude gradient in the endangered dioecious tree Taxus fuana Nan Li & R.R. Mill. Front Plant Sci. 2022;13:996750.
48. Niu F, He J, Zhang G, Liu X, Liu W, Dong M, Wu F, Liu Y, Ma X, An L, et al. Effects of enhanced UV-B radiation on the diversity and activity of soil microorganism of alpine meadow ecosystem in Qinghai-Tibet Plateau. Ecotoxicology. 2014;23(10):1833–41.
49. Zenoff VF, Heredia J, Ferrero M, Siñeriz F, Farías ME. Diverse UV-B resistance of culturable bacterial community from high-altitude wetland water. Curr Microbiol. 2006;52(5):359–62.
50. VanWallendael A, Benucci GMN, da Costa PB, Fraser L, Sreedasyam A, Fritschi F, Juenger TE, Lovell JT, Bonito G, Lowry DB. Host genotype controls ecological change in the leaf fungal microbiome. PLoS Biol. 2022;20(8):e3001681.
51. Guo Q, Zhu Y, Korpelainen H, Niinemets Ü, Li C. How does plant sex alter microbiota assembly in dioecious plants? Trends Microbiol. 2023;31(9):894–902.
52. Liu Q, Li L, Chen Y, Wang S, Xue L, Meng W, Jiang J, Cao X. Diversity of endophytic microbes in Taxus yunnanensis and their potential for plant growth promotion and taxane accumulation. Microorganisms. 2023;11(7):1645.
53. Xiong ZQ, Yang YY, Zhao N, Wang Y. Diversity of endophytic fungi and screening of fungal paclitaxel producer from Anglojap yew. Taxus x media BMC Microbiol. 2013;13:71.
54. Fu Y, Li X, Yuan X, Zhang Z, Wei W, Xu C, Song J, Gu C. Alternaria alternata F3, a novel taxol-producing endophytic fungus isolated from the fruits of taxus cuspidata: isolation, characterization, taxol yield improvement, and antitumor activity. Appl Biochem Biotechnol. 2023;196(4):2246–69.
55. Suryanarayanan TS, Ravishankar JP, Venkatesan G, Murali TS. Characterization of the melanin pigment of a cosmopolitan fungal endophyte. Mycol Res. 2004;108(Pt 8):974–8.
56. Semenzato G, Del Duca S, Vassallo A, Bechini A, Calonico C, Delfino V, Berti F, Vitali F, Mocali S, Frascella A, et al. Genomic, molecular, and phenotypic characterization of arthrobacter sp. OVS8, an endophytic bacterium isolated from and contributing to the bioactive compound content of the essential oil of the medicinal plant Origanum vulgare L. Int J Mol Sci. 2023;24(5):4845.
57 Xu D, Li N, Gu YQ, Huang J, Hu BS, Zheng JY, Hu JW, Du Q. Endophytic fungus Colletotrichum sp. AP12 promotes growth physiology and andrographolide biosynthesis in Andrographis paniculata (Burm. f.) Nees. Front Plant Sci. 2023;14:1166803.
58. Pan X, Li T, Liao C, Zhu Y, Yang M. The influences of fungal endophytes inoculation on the biochemical status of grape cells of different varieties in vitro. Plant Biotechnol (Tokyo). 2022;39(4):335–43.
59. Gupta DR, Khanom S, Rohman MM, Hasanuzzaman M, Surovy MZ, Mahmud NU, Islam MR, Shawon AR, Rahman M, Abd-Elsalam KA, et al. Hydrogen peroxide detoxifying enzymes show different activity patterns in host and non-host plant interactions with *Magnaporthe oryzae* Triticum pathotype. Physiol Mol Biol Plants. 2021;27(9):2127–39.
60. Yang R, Yang Y, Hu Y, Yin L, Qu P, Wang P, Mu X, Zhang S, Xie P, Cheng C, et al. Comparison of bioactive compounds and antioxidant activities in differentially pigmented *Cerasus humilis* fruits. Molecules. 2023;28(17):6272.

Publisher's Note